Centrifugal Drum Filtration: I. A Compression Rheology Model of Cake Formation

John D. Barr and Lee R. White
Chemical Engineering Dept., Carnegie Mellon University, Pittsburgh, PA 15213

DOI 10.1002/aic.10678
Published online September 29, 2005 in Wiley InterScience (www.interscience.wiley.com).

A compression rheology model is used to describe the behavior of networking solids undergoing centrifugal filtration under batch operation. A description of the batch filtration process is accomplished through the use of the rheologic functions for compressive yield stress $p_y(\phi)$ and the hydrodynamic resistance $R(\phi)$, with a characteristic pressure scaling, timescaling, and membrane resistance. Comparison of the results of this model to those found in engineering text books indicates that noncompression models fail to describe the variation in the cake resistance. The compression rheology model also predicts that the effective cake resistance is approximately 20% larger than that predicted by conventional theory. © 2005 American Institute of Chemical Engineers *AIChE J,* 52: 545–556, 2006

Keywords: centrifugal filtration, compression, cake formation

Introduction

Solid–liquid separations are fundamental to many industrial and laboratory processes. Filtration of compressible solid cakes has undergone examination in recent years by many researchers such as Tiller and coworkers,[1-5] as well as Wakeman[6] and others.[7-9] The models presented to date have relied on expressions of concentration and resistance as functions of pressure. We regard this methodology—although valid—as less representative of the local physical phenomena and so choose to use compression rheology to describe the relationship between pressure, solids concentration, and resistance.

The mathematical analysis of settling and consolidating solids, in particular flocculated solids, has had many contributors, including Bürger,[10-12] Buscall and coworkers,[13,14] and Landman and coworkers.[15-17] All apply a solids concentration diffusion model to the sedimentation and consolidation of the suspension and allow for local concentration, pressure, and resistance effects. These models are based on the observation that the solids network formed during filtration can be compacted (densified) under pressure and during an operation such as filtration the network density will change across the cross section of the cake of collected solids. This property is called *compressibility* and is not solely a property of flocculated suspensions; any material forming a space-filling network that densifies under pressure is compressible. This property complicates filtration because the resistance to liquid flow increases with the density of the cake. The physics of solids network compression has been widely analyzed.[7,13,18,19] We have adapted the compression rheology model used by Buscall and coworkers to the case of batch centrifugal filtration. This model describes the sedimentation, consolidation, and bed immobilization effects using a solids diffusion model for a plastically deforming solids network.

Mechanics of Separation

A force balance on the solids and liquid in an element of suspension with solids volume faction ϕ yields[19]

$$\nabla p_l = \phi R(\phi)(u - S) + \rho_l \boldsymbol{g} \tag{1}$$

$$\nabla p_s = -\phi R(\phi)(u - S) + \phi \Delta\rho \boldsymbol{g} \tag{2}$$

The suspension flux per unit area of filtration is

$$\boldsymbol{S} = \phi \boldsymbol{u} + (1 - \phi)\boldsymbol{w} \tag{3}$$

Correspondence concerning this article should be addressed to J. D. Barr at john.barr@gmail.com.

where

$$\nabla \cdot \boldsymbol{S} = 0 \tag{4}$$

where $\boldsymbol{u}$ is the solids velocity and $\boldsymbol{w}$ is the liquid velocity. Here $\Delta\rho = \rho_s - \rho_l$. $R(\phi)$ is the hydrodynamic resistance, an experimentally available function.[18,20] The function used in our present calculations is

$$R(\phi) = R_0(1 - \phi)^{(-5.5)} \tag{5}$$

which is comparable to the forms used by others.[15,18] For the purposes of this investigation, this function captures the essential functionality of the increase in resistance with increasing solids concentration. In practice, experiments would have to be conducted to determine the appropriate function for $R(\phi)$.[20,21]

The solids conservation equation is

$$\frac{\partial \phi}{\partial t} = -\nabla \cdot (\phi \boldsymbol{u}) \tag{6}$$

The force balance and solids conservation equation do not constitute a closed set of equations. We use the compressive rheology closure presented by Buscall and White[13]

$$p_s(\boldsymbol{r}, t) = p_y[\phi(\boldsymbol{r}, t)] \tag{7}$$

when the solids network is consolidating. If $p_s(\boldsymbol{r}, t) < p_y[\phi(\boldsymbol{r}, t)]$ then the network is strong enough to resist compression and becomes rigid. The compressive yield stress p_y is a measure of the mechanical strength of the solids network and is experimentally accessible.[13,21] The mechanical strength of the network vanishes below a critical volume fraction ϕ_g. For $\phi < \phi_g$, the solids are assumed to exist as isolated flocs and can therefore sustain no applied solids stress. The functional form of $p_y(\phi)$ used in these calculations is[14,22]

$$p_y(\phi) = p_0\left[\left(\frac{\phi}{\phi_g}\right)^5 - 1\right] \tag{8}$$

Centrifugal Filtration Model

The geometry of a centrifugal operation is necessarily cylindrical, with the outward radial direction being the primary direction of flow. For our problem we will require that the centrifuge operates uniformly around the circumference and along the length of the centrifuge, thus removing angular and axial dependency within the problem. We will consider the centrifugal force to greatly exceed any ordinary gravity contribution. The method of loading the centrifuge is crucial to the modeling of its operation. We choose to avoid as many complexities arising from start-up as possible and model a drum of radius r_m, spinning at constant speed ω (Hz), being instantaneously loaded with a volume per length v_0, of suspension with solids volume fraction ϕ_0 ($<\phi_g$). Under these conditions, centrifugal drum filtration becomes a two-dimensional problem in the radial coordinate r and time t, once turbulence and edge effects have been neglected for a uniformly loaded drum.

The total filtrate volume expressed per unit length of the centrifuge is $v(t)$. During filtration $v \geq 0$, $\dot{v} > 0$, and $\ddot{v} < 0$. From Eq. 3

$$S(r, t) = \frac{\dot{v}(t)}{2\pi r} \tag{9}$$

The "weight" term $\boldsymbol{g}$, in Eqs. 1 and 2, is just the centrifugal acceleration, $\boldsymbol{g} = \omega^2 r \hat{\boldsymbol{r}}$. The force balances become

$$\frac{\partial p_s}{\partial r} = \Delta\rho\phi\omega^2 r - R(\phi)\left(\phi \boldsymbol{u} - \frac{\phi\dot{v}}{2\pi r}\right) \tag{10}$$

$$\frac{\partial p_l}{\partial r} = \rho_l\omega^2 r + R(\phi)\left(\phi \boldsymbol{u} - \frac{\phi\dot{v}}{2\pi r}\right) \tag{11}$$

The total pressure, $p_t = p_s + p_l$ obeys

$$\frac{\partial p_t}{\partial r} = (\Delta\rho\phi + \rho_l)\omega^2 r \tag{12}$$

Integrating Eq. 12 from the top of the suspension to the membrane yields

$$p_t(r_m, t) = p_a + \frac{\rho_l\omega^2}{2\pi}\left(1 + \frac{\Delta\rho}{\rho_l}\phi_0\right)v_0 - \frac{\rho_l\omega^2}{2\pi}v \tag{13}$$

and at the membrane ($r = r_m$)

$$p_l(r_m, t) = \frac{R_{mem}}{2\pi r_m}\dot{v}(t) + p_a \tag{14}$$

where R_{mem} is the membrane resistance per unit length and p_a is the ambient pressure. Thus

$$p_s(r_m, t) = \rho_l\omega^2\left(1 + \frac{\Delta\rho}{\rho_l}\phi_0\right)\frac{v_0}{2\pi} - \frac{\rho_l\omega^2}{2\pi}v(t) - \frac{R_{mem}}{2\pi r_m}\dot{v}(t) \tag{15}$$

Initially, the solids pressure at the membrane is zero because material has just started to accumulate [$\phi(r_m, 0) = \phi_g$] and $\dot{v}$ is at its maximum, at $v = 0$ (see Eq. 15). As material accumulates and the cake grows, the concentration at the membrane will increase as the solids are compacted into structures that can support the greater solids stress. The solids concentration at the membrane will reach a maximum at the time t_l (see Figure 1) where the solids pressure at the membrane is maximal. From Eq. 15 we see that $\phi(r_m, t)$ reaches its maximum when

$$\frac{\rho_l\omega^2}{2\pi}\dot{v}(t_l) = -\frac{R_{mem}}{2\pi r_m}\ddot{v}(t_l) \tag{16}$$

Thus there are two timescale regimes within the problem: a membrane resistance controlled regime (Initial Cake Formation) and a cake resistance controlled regime (Cake Growth). In the membrane resistance controlled regime, the concentration at the membrane is increasing. After the concentration at the

membrane has reached its maximum, the cake resistance controls the timescale.

Note that, although the concentration at the membrane is increasing, the total pressure at the membrane has been decreasing as a result of removal of fluid from the centrifuge (see Figure 1). The decreasing total pressure produces an effect called "cake immobilization," a phenomenon first reported by Sambuichi.[1] Under conditions of decreasing total pressure, for $t > t_I$ the solids pressure will drop below the yield stress in compacted portions of the cake closest to the membrane. The result is that an immobilized zone, $r_m \le r \le r_I(t)$, moves inward from the membrane for $t > t_I$, in which the solids network is no longer consolidating.

Moving Boundaries

In addition to the membrane at $r = r_m$, there are up to four more internal boundaries in the problem (see Figure 2). These boundaries are mobile and correspond to transitions in the behavior of the solids. The inner fluid surface $r_f(t)$, the interior boundary of the supernatant layer, is given by

$$(1 - \phi_0)v_0 - v(t) = 2\pi \int_{r_m}^{r_f} (1 - \phi) r dr \tag{17}$$

A clear supernatant layer $r_f(t) \le r < r_s(t)$ will form at the inner surface as a result of the density difference between the liquid and solids. The boundary between the clear supernatant and the sedimenting zone is $r_s(t)$. Within the sedimenting zone isolated particles and flocs are driven toward the membrane by both convection and centrifugal gravity. Here the particle stress is zero because the volume fraction is below ϕ_g.

The inner surface of the cake is $r_c(t)$. At the cake surface the sedimenting solids are collected into stress-supporting structures at the gel point $[\phi(r_c^+, t) = \phi_g]$, which are in turn compressed by new material convecting into the cake. This produces a region of consolidating networked solids in which the solids flux, from Eqs. 2 and 7, is

$$\phi \boldsymbol{u} = \Delta\rho\omega^2 r \frac{\phi}{R(\phi)} + \frac{\phi \dot{v}}{2\pi r} - D(\phi)\frac{\partial \phi}{\partial r} \tag{18}$$

where $D(\phi)$ is the solids diffusion coefficient[22]:

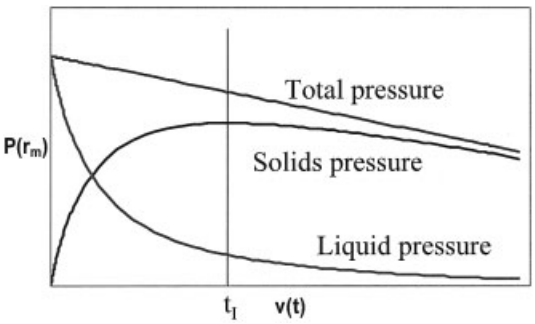

Figure 1. Pressure at membrane as filtration proceeds.

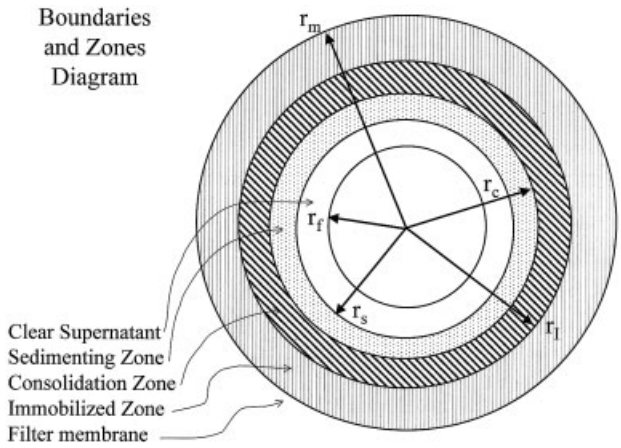

Figure 2. Centrifuge cross section.

$$D(\phi) = \frac{\partial p_y(\phi)}{\partial \phi} \Big/ R(\phi) \tag{19}$$

The boundary $r_c(t)$ is a discontinuity in ϕ and the solids flux, given that $\phi(r_c^-, t) < \phi_0$. The compressing cake occupies $r_c(t) \le r < r_I(t)$ and the immobilized zone occupies $r_I(t) \le r \le r_m$ $(t > t_I)$ as discussed above.

Because there is no mechanism for a discontinuity in concentration to develop at $r_I(t)$ it follows that the solids flux must be continuous across $r_I(t)$ and the immobilization boundary is not a first-order shock. Initially, $r_I(t) = r_m$ $(t \le t_I)$ as the solids collect at the membrane that serves as the zero solids flux boundary. At $t = t_I$, $p_s(r_m)$ will reach a maximum (see Figure 1), and the zero solids flux boundary $r_I(t)$ will move away from the wall at subsequent times.

While $r_f(t) < r_c(t)$ the cake is saturated and $p_l(r_f, t) = p_a$. Thus Eq. 17 becomes

$$\pi(r_m^2 - r_f^2) = v_0 - v(t) \tag{20}$$

In this case, integrating Eq. 11 from $r_f(t)$ to r_m yields

$$\dot{v} = \frac{\rho_l \omega^2 (r_m^2 - r_f^2) + S_s + S_c}{\dfrac{R_{mem}}{\pi r_m} + \int_{r_c}^{r_m} dr \dfrac{\phi R(\phi)}{\pi r}} \tag{21}$$

where

$$S_s = \Delta\rho\omega^2 \phi_s(t)(r_c^2 - r_s^2) \tag{22}$$

$$S_c = 2\int_{r_c}^{r_m} dr \phi u R(\phi) \tag{23}$$

Here we have used Eq. 10 with $p_s = 0$ to eliminate the solids flux in the sedimenting zone. The first term in the numerator of Eq. 21 is the fluid contribution to the driving force and the remaining two terms represent the solids contribution in the sediment (S_s) and cake (S_c).

Scaling the Centrifugal Model

We choose the following scalings:

$$P = \frac{2p}{\rho_l \omega^2 r_m^2} \qquad T = \frac{t}{t^*} \qquad \lambda = \frac{R(\phi)}{R^*} \qquad V = \frac{v}{\pi r_m^2}$$
$$Z = \frac{r_m^2 - r^2}{r_m^2} \qquad \Delta(\phi) = D(\phi)\,\frac{2R^*}{\rho_l \omega^2 r_m^2} \qquad \psi = \frac{2t^*}{r_m^2}\, r\phi u \tag{24}$$

where t^* and R^* are chosen so that

$$\frac{2\rho_l \omega^2 r_m^2 t^*}{R^* r_m^2} = 1 \qquad t^* = \frac{R^*}{2\rho_l \omega^2} \tag{25}$$

Conservation of solids (Eq. 6) becomes

$$\frac{\partial \phi}{\partial T} = \frac{\partial \psi}{\partial Z} \tag{26}$$

The scaled solids flux, from Eq. 18, becomes

$$\psi(Z, T) = \phi \dot{V} + (1 - Z)\left[\frac{\Delta\rho}{\rho_l}\frac{\phi}{\lambda} + \Delta(\phi)\frac{\partial \phi}{\partial Z}\right] \tag{27}$$

and Eq. 15 yields

$$P_s(0, T) = L\left(1 + \frac{\Delta\rho}{\rho_l}\phi_0\right) - V - \mu \dot{V} \tag{28}$$

where

$$\mu = \frac{2R_{mem}}{R^* r_m} \qquad L = \frac{v_0}{\pi r_m^2} \tag{29}$$

This scaling leaves us with a degree of freedom, allowing us to specify a time or resistance scaling. In the initial stage of cake formation the rate of expression is controlled by the membrane resistance and in this portion of the process we choose to specify the resistance scaling, R^*, so that $\mu = 1$, and thus

$$R^* = \frac{2R_{mem}}{r_m} \qquad \text{for} \qquad T \le T_l \tag{30}$$

For $T > T_l$, the cake will be the controlling resistance. Accordingly the resistance scaling R^* is reset to promote total filtration in $O(1)$ scaled time (see below). We define

$$I_1(Z) = \int_0^Z \phi dZ \tag{31}$$

$$I_2(Z) = \int_0^Z \frac{\phi\lambda}{1 - Z}\, dZ \tag{32}$$

$$I_3(Z) = \int_{Z_l}^Z \frac{\psi\lambda}{1 - Z}\, dZ \tag{33}$$

Thus Eqs. 20 and 21 become, respectively,

$$\dot{V}(T) = \frac{Z_f(T) + \frac{\Delta\rho}{\rho_l}\phi_s(T)(Z_s - Z_c) + I_3(Z_c)}{\mu + I_2(Z_c)} \tag{34}$$

$$Z_f(T) = L - V(T) \tag{35}$$

Solution Zones

Sedimenting zone

In the sedimenting zone, Eq. 27 reduces to

$$\psi_s(Z, T) = \phi \dot{V} + (1 - Z)\left[\frac{\Delta\rho}{\rho_l}\frac{\phi}{\lambda(\phi)}\right] \tag{36}$$

Substituting this into the continuity equation (Eq. 26) yields a first-order partial differential equation that can be solved using the *method of characteristics*[23] to yield $\phi(Z, T) = \phi_s(T)$ where

$$\frac{\partial \phi_s}{\partial T} = -\frac{\Delta\rho}{\rho_l}\frac{\phi_s}{\lambda(\phi_s)} \qquad (Z_c^+ \le Z \le Z_s) \tag{37}$$

and $Z_s(T)$, where

$$[1 - Z_s(T)]\phi_s - (1 - L)\phi_0 = \int_0^T dT \phi_s \dot{V} \tag{38}$$

At $T = T_s$ the sedimenting zone disappears into the cake, $Z_s(T_s) = Z_c(T_s)$, and cake formation is complete. The supernatant, $Z_c < Z \le Z_f$ will continue to drain through the cake until T_c at which $Z_c(T_c) = Z_f(T_c)$. Subsequent cake compression and drainage ($T > T_c$) behavior requires additional physics and is the subject of a second article.[24]

Consolidation zone

In this region, ψ is given by Eq. 27 and, when substituted in Eq. 26, produces a diffusion equation for $\phi(Z, T)$, which must be solved subject to appropriate boundary conditions. Howells and coworkers[15] presented a numerical algorithm for this form of equation using a backwards-difference approximation for $\partial\phi/\partial T$. Attempts to numerically solve the consolidation equations with the backwards-difference approximation for $\partial\phi/\partial T$ in the cake growth region proved inaccurate as a result of the initial magnitude of $\partial\phi/\partial T$. This difficulty is circumvented as follows. We define

Table 1. System Values and Functions Used in Centrifugal Filtration Calculations

Drum radius	$r_m = 1.0$ m	Initial load	$r_f(0) = 0.5$ m
Density of liquid	$\rho_l = 1.0$ g/cm^3	Density of solids	$\rho_s = 2.0$ g/cm^3
Initial solids volume fraction	$\phi_0 = 0.1$	Gel point	$\phi_g = 0.15$
Compressive yield stress	$p_y(\phi) = p_0[(\phi/\phi_g)^5 - 1]$	Scaled initial load	$L = 0.75$
Hydrodynamic resistance	$R(\phi) = R_0(1 - \phi)^{-5.5}$	Liquid viscosity	$\mu_f = 0.001$ kg m^{-1} s^{-1}

$$q = \Delta(\phi)\frac{\partial \psi}{\partial Z} = \Delta(\phi)\frac{\partial \phi}{\partial T} \tag{39}$$

Differentiating Eq. 27 with respect to T and using the definition of q, we obtain the following coupled equation set:

$$\begin{aligned}
\frac{\partial \phi}{\partial Z} &= -\frac{1}{\Delta(\phi)}\left(\frac{\phi \dot{V}}{1-Z} + \frac{\Delta\rho}{\rho_l}\frac{\phi}{\lambda} - \frac{\psi}{1-Z}\right) \\
\frac{\partial \psi}{\partial Z} &= \frac{q}{\Delta(\phi)} \\
\frac{\partial q}{\partial Z} &= -\frac{1}{\Delta(\phi)}\left\{q\left[\frac{\dot{V}}{1-Z} + \frac{\Delta\rho}{\rho_l}\left(\frac{\phi}{\lambda}\right)'\right]\right\} \\
&\quad - \frac{1}{1-Z}\left(\phi \ddot{V} - \frac{\partial \psi}{\partial T}\right)
\end{aligned} \tag{40}$$

where the time derivative $\partial\psi/\partial T$ can now be replaced by a backwards difference with little error because $\psi(Z, T)$ is small in the cake.

The boundary conditions are[25]

$$\psi(Z_I, T) = 0 \qquad \phi(Z_c^-) = \phi_g \qquad (Z_c < Z_f) \tag{41}$$

$$q(Z_I, T) = \begin{cases} -\dfrac{\dot{V} + \mu \ddot{V}}{\lambda[\phi(0, T)]} & (T \le T_I) \\ 0 & (T > T_I) \end{cases} \tag{42}$$

The cake boundary obeys a shock equation[23]

$$\dot{Z}_c(T) = \frac{\psi_s(Z_c^+, T) - \psi(Z_c^-, T)}{\phi_g - \phi_s(T)} \tag{43}$$

where $\psi(Z_c^-, T)$, the flux just inside the cake, is determined by solving the Eq. 40 set.

Immobilized zone

Integrating Eq. 10 through the immobilization zone ($\psi = q = 0$) from $Z = 0$ to the start of the compression zone [$Z = Z_I(T)$], and using Eq. 15, yields the scaled equation

$$\begin{aligned}
P_s(Z_I, T) = P_y(\phi_I) &= L\left(1 + \frac{\Delta\rho}{\rho_l}\phi_0\right) \\
&\quad - V - \dot{V}[\mu + I_2(Z_I)] - \frac{\Delta\rho}{\rho_l} I_1(Z_I)
\end{aligned} \tag{44}$$

where $\phi_I(T) = \phi(Z_I^+, T)$. Differentiating this equation with respect to T yields

$$q(Z_I, T) = -\frac{\dot{V} + \ddot{V}[\mu + I_2(Z_I)]}{\lambda(\phi_I)} \tag{45}$$

Note that Eq. 45 reduces to the $q(0, T)$ boundary condition (Eq. 42) for $T \le T_I$ where $Z_I(T) = 0$. Both ψ and q must be continuous at $Z = Z_I(T)$ so that

$$\dot{V} + \ddot{V}[\mu + I_2(Z_I)] = 0 \qquad (T \ge T_I) \tag{46}$$

This serves to determine $\ddot{V}$ once $\dot{V}$ is specified for $T > T_I$.

Initial Cake Formation—Stage 1

The initial period of cake formation can be <1% of the total filtration time, although this small period can greatly influence later behavior because the volume fraction at and near the membrane is determined during this period.

Calculations were carried out using a FORTRAN program[25] using the model properties detailed in Table 1. The control parameters of the system are

$$\mathsf{M} = \frac{R_{mem}}{R_0} \qquad \mathsf{P}* = \frac{\rho_l \omega^2 r_m^2}{2p_0} \tag{47}$$

For brevity, functions of ϕ are notated $F_i = F(\phi_i)$.

Small time solution

At $T = 0^+$ an infinitely thin layer of cake at volume fraction ϕ_g ($p_s = 0$) forms at the membrane. As filtrate is expressed this layer will grow in density and thickness. We use a Taylor expansion technique to determine the initial values of $\dot{V}$, $\ddot{V}$, and $\dot{Z}_c$.[25]

$$\dot{V}(0^+) = L\left(1 + \frac{\Delta\rho}{\rho_l}\phi_0\right) \tag{48}$$

$$\dot{Z}_c(0^+) = \frac{\dot{V}(0^+)\phi_0 + \dfrac{\Delta\rho}{\rho_l}\left(\dfrac{\phi}{\lambda}\right)_0}{\phi_g - \phi_0} \tag{49}$$

$$\ddot{V}(0^+) = -\dot{V}(0^+)\left[1 + \frac{\phi_g \phi_0 \lambda_g L}{\phi_g - \phi_0}\dot{V}(0^+)K_0 K_g\right] \tag{50}$$

where

$$K_i = \left[1 + \frac{\dfrac{\Delta\rho}{\rho_l}}{\lambda_i \dot{V}(0^+)} \right] \tag{51}$$

Subsequently, Eq. 45 determines $q(0, 0^+)$.

Cake formation algorithm

The solids flux gradient at the membrane, $q(0^+, T)$, is initially very large and decreases to zero when the cake at the membrane immobilizes ($T = T_I$). To calculate the time evolution of the filtration, we systematically vary $q[0, T^{(k)}]$ from $q(0, 0^+)$ to zero in a set of steps corresponding to times $T^{(k)}$ ($k = 1, 2, \ldots, N$). At each step, we guess $\dot{V}^{(k)}$ [$<\dot{V}^{(k-1)}$] and use Eq. 45 to determine $\ddot{V}^{(k)}$. The time step $\Delta T^{(k)} = T^{(k)} - T^{(k-1)}$ is calculated from

$$\Delta T^{(k)} = 2\Delta\dot{V}^{(k)}/[\ddot{V}^{(k)} + \ddot{V}^{(k-1)}] + \cdots \tag{52}$$

and the volume step $\Delta V^{(k)}$ from

$$\Delta V^{(k)} = \Delta\dot{V}^{(k)} \frac{\dot{V}^{(k-1)} + \dot{V}^{(k)}}{\ddot{V}^{(k-1)} + \ddot{V}^{(k)}} + \cdots \tag{53}$$

accurate to cubic order in $\Delta\dot{V}^{(k)}$. We then determine $\phi[0, T^{(k)}]$ from Eq. 44 and $\phi_s^{(k)}$ and $Z_s^{(k)}$ from Eqs. 37 and 38. The consolidation equation set 40 is solved numerically from $Z = 0$ to Z^*, where $\phi(Z^*) = \phi_g$ using a fourth-order Runge–Kutta method with step-size control.[26] For $Z > Z_c^{(k-1)}$, we extrapolate $\psi[Z, T^{(k-1)}]$ using a Taylor series.[22]

To verify our estimate for $\dot{V}^{(k)}$ we calculate

$$Z_c^{(k)} = Z_c^{(k-1)} + \frac{\Delta T^{(k)}}{2} (\dot{Z}_c^{(k)} + \dot{Z}_c^{(k-1)}) + \cdots \tag{54}$$

and accept $\dot{V}^{(k)}$ if

$$1 - Z^*/Z_c^{(k)} < \text{tolerance} \qquad (1.0 \times 10^{-5}) \tag{55}$$

To determine $\dot{Z}_c^{(k)}$ we have the shock Eq. 43 and, from $\phi(Z_c^-, T) = \phi_g$, we obtain, by differentiation with respect to T,

$$\dot{Z}_c = -q(Z_c^-, T) \Big/ \left(\Delta_g \frac{\partial\phi}{\partial Z} (Z_c^-, T) \right) \tag{56}$$

Because $\psi[Z, T^{(k)}]$ and $q[Z, T^{(k)}]$ are least accurately determined around $Z_c^{(k)}$, it was found convenient to determine $\dot{Z}_c$ by a suitable average of Eqs. 43 and 56,[25] which minimized this solution error. If Eq. 55 is not satisfied, we choose another $\dot{V}$ and reiterate step k until the set tolerance is achieved.

Small time solution for zero membrane resistance

In the limit of $\mathsf{M} = 0$, we can derive a small T similarity solution[25]

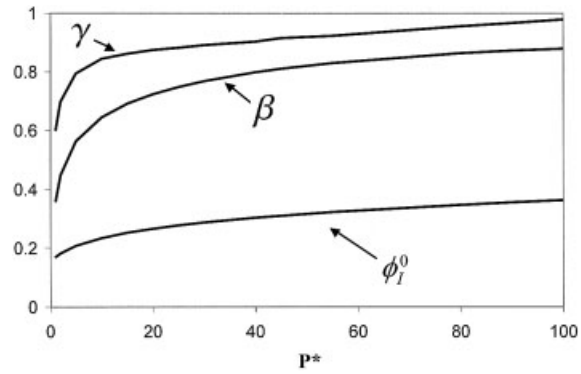

Figure 3. Zero membrane resistance centrifugal similarity solution parameters.

$$\phi(Z, T) = \Phi(Z/Z_c) \qquad \eta = Z/Z_c \qquad V = \beta\sqrt{T}$$
$$Z_c = \gamma\sqrt{T} \qquad Z_I = \frac{2}{\phi_I^0 \lambda(\phi_I^0)} T \tag{57}$$

where β and γ are constants to be determined. The membrane solids concentration ϕ_I^0 is given by

$$P_y(\phi_I^0) = L\left(1 + \frac{\Delta\rho}{\rho_l} \phi_0 \right) \tag{58}$$

The similarity differential equation is

$$\frac{d}{d\eta}\left[\Delta(\Phi) \frac{d\Phi}{d\eta} \right] + \frac{1}{2} (\gamma^2\eta + \gamma\beta) \frac{d\Phi}{d\eta} = 0 \tag{59}$$

with boundary conditions

$$\Phi(0) = \phi_I^0 \qquad \frac{d\Phi}{d\eta}(0) = -\frac{\beta\gamma}{2} \frac{\phi_I^0}{\Delta(\phi_I^0)}$$
$$\Phi(1) = \phi_g \qquad \frac{d\Phi}{d\eta}(1) = -\frac{\phi_g - \phi_0}{2\Delta_g} \gamma(\gamma + \beta) \tag{60}$$

These four boundary conditions are sufficient to solve Eq. 59 and thus determine β and γ. The solution algorithm is discussed by Barr.[25] $R^* = \rho_l\omega^2 r_m^2/[2D(\phi_I^0)]$. Values of γ, β, and ϕ_I^0 as functions of P^* for the model system given in Table 1 are plotted in Figure 3.

Numerical Results—Stage 1

$\phi(0, t)$

As discussed earlier for nonzero membrane resistances, the concentration at the membrane increases until a maximum is reached at t_I. The concentration at t_I depends strongly on P^* and M as shown in Figures 4 and 5, with concentrations at the membrane approaching the theoretical maximum (ϕ_I^0) as M decreases. In these figures, we have unscaled the time variable ($R_0 = 4.486 \times 10^6$ kPa·s/m^2; thus all times are in seconds) for comparison purposes. For clarity in Figure 4 we do not exhibit the zero membrane resistance results for other than $\mathsf{P}^* = 100$.

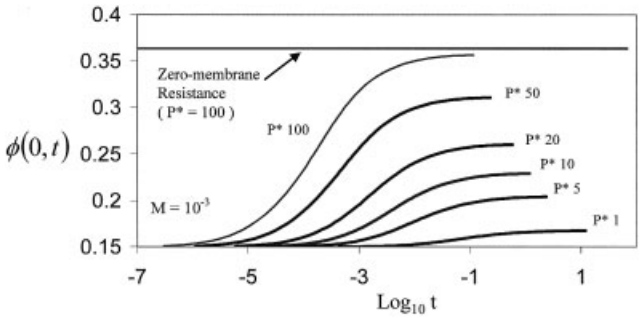

Figure 4. $\phi(0, t)$ for $0^+ < t \leq t_I$ (seconds) at M = 0.001.

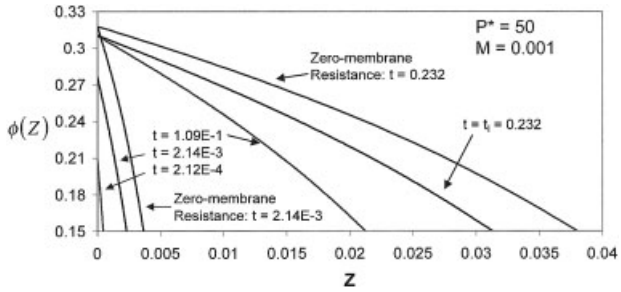

Figure 6. $\phi(Z, t)$ evolution at P* = 50 and M = 0.001.
Time is expressed in seconds.

$\phi(Z, t)$ profiles

In Figure 6 we plot $\phi(Z, t)$ as a function of Z for $P^* = 50$, $M = 10^{-3}$, and various unscaled times t. The zero membrane resistance case evaluated at t_I shows a cake profile comparable to the small membrane resistance calculation at the same time.

At large membrane resistance we observe substantial deviation from the zero membrane resistance solution as expected (see Figure 7). Figure 7 shows a case where the sedimenting solids have been completely absorbed by the cake before the cake at the membrane immobilizes ($t_s < t_I$). Note that there is little difference between the profiles at t_s and t_I in this case. This situation occurs for large membrane resistance and small driving pressures where sedimentation is complete before the solids pressure at the membrane peaks.

Expressed volume, V(t)

Figures 8 and 9 show the scaled filtrate volume expressed over time. As with $\phi(0, t)$, the full numeric solution approaches the zero membrane resistance solution as $M \rightarrow 0$ once a substantial cake has developed, as shown in Figure 8. Figure 9 shows that the volume expressed at t_I is relatively constant for a given M and that the applied pressure controls t_I.

All the solutions displayed in Figure 9 tend toward the zero membrane resistance behavior, which is consistent with the resistance of the forming cake becoming dominant over the membrane resistance contributions. The $M = 0.1$ case is different in that the time to the onset of immobilization is so much greater than that for the smaller resistances that the cake is fully formed before the onset of immobilization ($t_s < t_I$). Note that $L(1 - \phi_0) = 0.675$ in these calculations so that a very small fraction of the total fluid has been expressed at $t = t_I$.

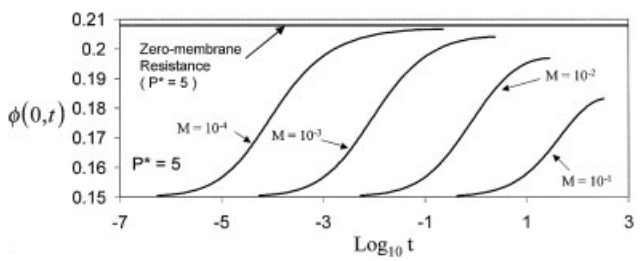

Figure 5. $\phi(0, t)$ for $0^+ < t \leq t_I$ (seconds) at P* = 5.

Ratio of membrane to cake resistance

The ratio of liquid pressure drop across the membrane to liquid pressure drop arising from cake resistance is

$$\text{Ratio} = \frac{\mu \dot{V}}{P_y[\phi(0, T)] + \dfrac{\Delta\rho}{\rho_l}[\phi_0 L - \phi_s(Z_s - Z_c)]} \tag{61}$$

In Figure 10 we show that, initially, even for small values of membrane resistance, the membrane resistance is several orders of magnitude greater than the cake resistance. As the cake approaches the start of immobilization the ratio inverts. Accordingly we revert to the cake as the controlling resistance with the onset of immobilization.

Bed Immobilization—Stage 2

For $T > T_I$ we rescale all variables using

$$R^* = \frac{\rho_l \omega^2 r_m^2}{2D[\phi(0, T_I)]} \tag{62}$$

so as to produce $\Delta(\phi)$ as an $O(1)$ quantity and μ is now given by Eq. 29. Note that the initial cake growth, which produces $\phi(0, T_I)$ and thus the cake resistance, controls the overall filtration time.

Solving the differential equations during bed immobilization is functionally the same as during initial cake formation, except that Z_I^k must be determined before the consolidation equations can be solved. First, the concentration at the immobilization boundary $\phi_I^{(k)}$ [$<\phi_I^{(k-1)}$] is chosen. With a guess for $\dot{V}^{(k)}$, Eqs.

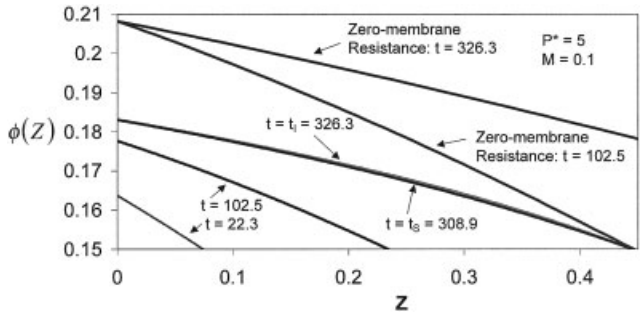

Figure 7. $\phi(Z, t)$ evolution at P* = 5 and M = 0.1.
Time is expressed in seconds.

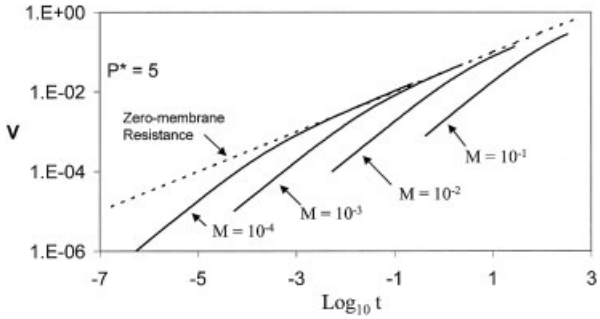

Figure 8. Volume expressed for $t \le t_I$ (seconds) at P* = 5.

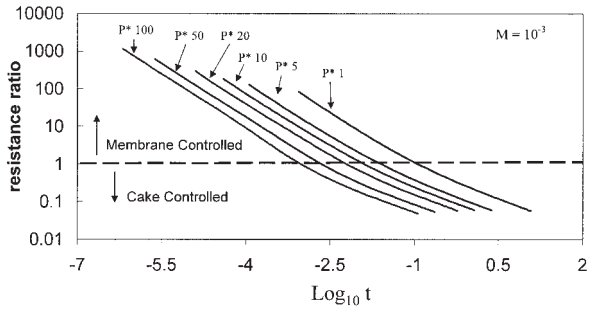

Figure 10. Ratio of membrane resistance to cake resistance for $t \le t_I$ (seconds) at $M = 0.001$.

53, 46, 52, and 44 can be solved iteratively for $\Delta V^{(k)}$, $\dot{V}^{(k)}$, $\Delta T^{(k)}$, and $\Delta Z_I^{(k)}$ where we use

$$I_j[Z_I^{(k)}] = I_j[Z_I^{(k-1)}] + \Delta Z_I^{(k)} A_j + \cdots \tag{63}$$

accurate to cubic order in $\Delta Z_I^{(k)}$ and

$$A_1 = \frac{\phi_I^{(k)} + \phi_I^{(k-1)}}{2} \tag{64}$$

$$A_2 = \frac{1}{2}\left[\left(\frac{\phi_I \lambda_I}{1 - Z_I}\right)^{(k)} + \left(\frac{\phi_I \lambda_I}{1 - Z_I}\right)^{(k-1)}\right] \tag{65}$$

If $\Delta Z_I^{(k)}$ and $\Delta V^{(k)}$ are sufficiently small we can proceed to solve Eqs. 37 and 38 for $\phi_s^{(k)}$ and $Z_s^{(k)}$ and then solve the consolidation Eq. 40 set subject to Eqs. 41 and 42 as in initial cake formation. The validity of our guess for $\dot{V}^{(k)}$ is determined as described previously.

End of sedimentation

For $T \ge T_s$ the sedimentation zone vanishes and Eq. 43 becomes

$$\dot{Z}_c(T) = -\psi(Z_c^-, T)/\phi_g < 0 \tag{66}$$

All solids are now collected in the cake and no weight is being added at the cake surface. The weight increase as the cake forms serves to keep $\dot{Z}_I$ relatively small. Once this is not present, $\dot{Z}_I$ accelerates as the outward hydrodynamic drag decreases with $\dot{V}$. The Stage 2 solution algorithm outlined above becomes unwieldy as $\Delta Z_I^{(k)}$ becomes increasingly large. It thus becomes necessary to assume that the entire cake has immobilized once $Z_I[T^{(k-1)}]$ is acceptably close to $Z_c[T^{(k-1)}]$ and the solids flux, $\psi[Z_c, T^{(k-1)}]$, has reached zero to within a set tolerance. The next time step to $T^{(k)} = T_c$ is taken by assuming

$$Z_c(T) = Z_c^{(k-1)} \qquad \phi(Z, T) = \phi[Z, T^{(k-1)}] \tag{67}$$

for $T^{(k-1)} \le T \le T_c$. Equation 34 reduces to

$$\dot{Z}_f = -Z_f/[\mu + I_2(Z_c)] \tag{68}$$

which integrates to yield $Z_f(T)$ given that Z_c is fixed. The time T_c is determined by $Z_f(T_c) = Z_c^{(k-1)}$ and is given by

$$\frac{T_c - T^{(k-1)}}{\mu + I_2(Z_c[T^{(k-1)}])} = \ln\left(\frac{Z_f[T^{(k-1)}]}{Z_c[T^{(k-1)}]}\right) \tag{69}$$

We then solve for $V(T_c)$, $\dot{V}(T_c)$, and $\ddot{V}(T_c)$. Thus the state of the system at the end of cake formation is determined and serves as the starting state of the subsequent compression and drainage stages reported elsewhere.[24,25]

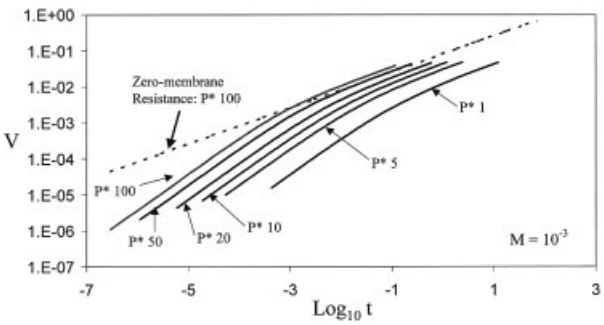

Figure 9. Volume expressed for $t \le t_I$ (seconds) at $M = 0.001$.

The similarity solution is shown out to maximum possible expression.

Numerical Results—Stage 2

$\phi_I(t)$ at immobilization front

In Figure 11 we plot the solids concentration at the immo-

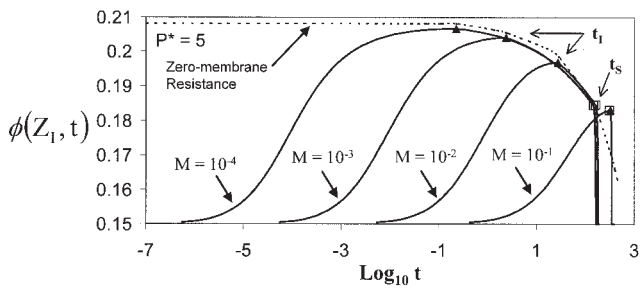

Figure 11. Solids concentration for $0 \le t \le t_c$ (seconds) at $Z_I(t)$ for $P^* = 5$.

t_I and t_s are marked on each plot.

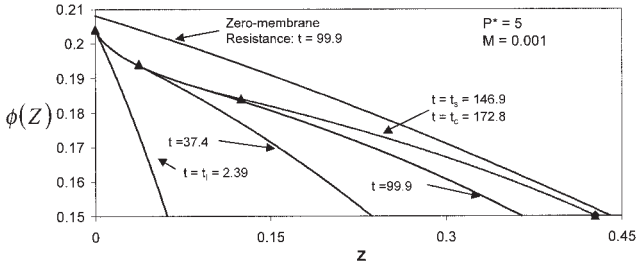

Figure 12. Solids concentration profiles for P* = 5 and M = 0.001 for $t_l \le t \le t_c$ (seconds).

The position of $Z_l(t)$ is marked on each profile.

bilization boundary [$\phi_l(t)$] as a function of unscaled time for various membrane resistances at P* = 5. It is clear that t_l increases with membrane resistance and $\phi_l(t)$ decreases. However, after t_l, as the immobilization zone moves away from the membrane, the $\phi_l(t)$ curve appears to be invariant with membrane resistance for the smaller membrane resistances shown. This results from the cake resistance domination of the filtration after t_l. The M = 0 similarity solution predicts

$$\phi_l^{sim}(t) = \Phi\left[\frac{2\sqrt{T}}{\phi_l^0 \lambda(\phi_l^0)\gamma}\right] \tag{70}$$

and this curve is also plotted in Figure 11. Note that it is a reasonable estimate of $\phi_l(t)$ for small M.

At small membrane resistances a significant amount of solids have yet to be collected into the network when the immobilization process starts, so rapid immobilization does not set in until the solids network is fully formed at t_s. At large membrane resistances the cake is nearly fully formed when the immobilization process starts, resulting in rapid immobilization of the network.

ϕ(Z, t) during cake growth

In Figures 12 and 13 we show cake profiles at various unscaled times up to t_c for small M values. For large membrane resistances the cake is nearly fully formed at t_l and later profiles are essentially indistinguishable from the solids concentration profile at t_c and are not plotted here.[25] At small values of M significant quantities of solids are still in the sedimenting zone at t_l and so the cake undergoes the bulk of its growth in this stage of calculation for these values of M. We observe that the

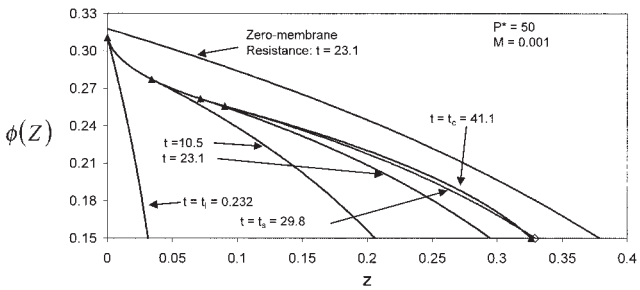

Figure 13. Solids concentration profiles for P* = 50 and M = 0.001 for $t_l \le t \le t_c$ (seconds).

The position of $Z_l(t)$ is marked on each profile.

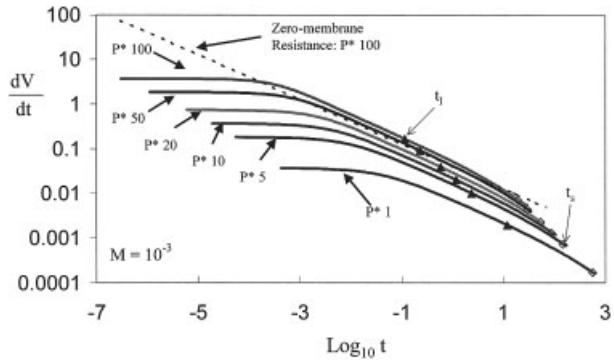

Figure 14. Rate of expression in cake formation at M = 0.001 and $0 \le t \le t_c$ (seconds).

t_l and t_s are marked on each plot.

zero membrane resistance solution consistently overpredicts the cake thickness at t_c.

V̇(t) and V(t) during cake growth

In Figures 14 and 15 we plot $\dot{V}(t)$ and $V(t)$ for M = 0.001 and various values of P*. At least for small M, the plots are insensitive to M as expected. We observe that $\dot{V}(t)$ and $V(t)$ for a given P* approach the corresponding similarity solution result. We show the similarity solution results for P* = 100 in the figures but have omitted the similarity results for other pressures for clarity. It is somewhat surprising that the similarity solution produces such close comparisons because it is strictly a small time solution only.

Comparison with Conventional Model

The conventional theory of pressure and centrifugal filtration[27-29] assumes that the cake resistance per unit solids mass α is a constant throughout the cake formation stage and that the cake is immobile. In constant pressure filtration, the conventional model predicts that a plot of t/v vs. v is linear and that the slope of that plot is proportional to α. Thus laboratory pressure filtration studies allow $\alpha(\Delta p)$ to be extracted, where Δp is the applied piston pressure. We denote the pressure filter measured quantity $\alpha_p(\Delta p)$. The compression rheology model of pressure filtration also predicts the linearity of a t/v vs. v plot using $R(\phi)$ and $p_y(\phi)$ as the fundamental suspension properties. Accord-

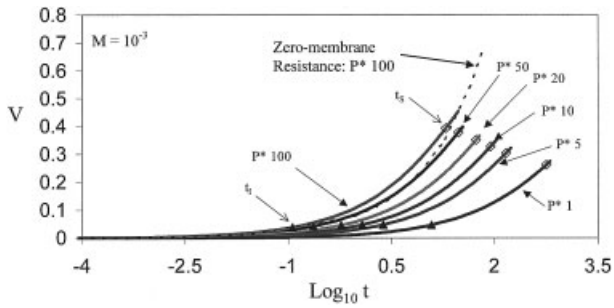

Figure 15. Volume expressed during cake formation at M = 0.001 and $0 \le t \le t_c$ (seconds).

t_l and t_s are marked on each plot. The similarity solution is shown out to maximum possible expression.

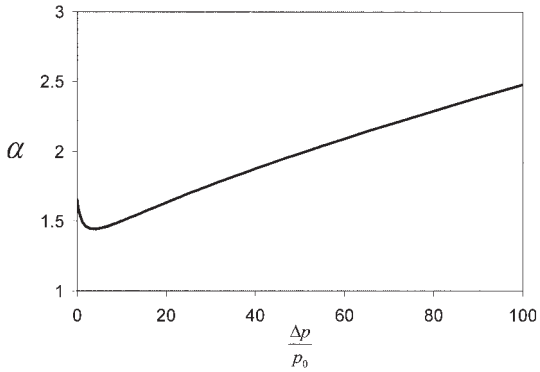

Figure 16. Cake resistance (10^{10} m/kg) for model system under pressure filtration.

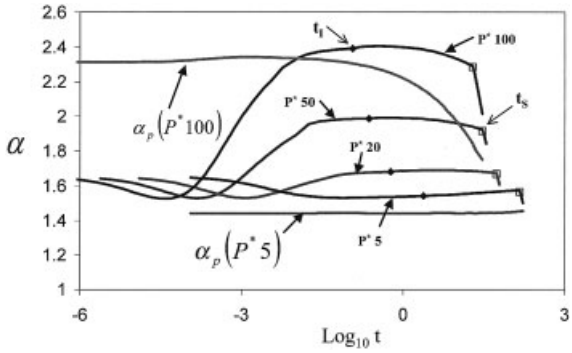

Figure 17. α_c and α_p (10^{10} m/kg) for $0 < t \le t_c$ (seconds) and $M = 10^{-3}$.

$\alpha_c^{sim} = 4.7 \times 10^{10}$ m/kg for P* = 100 (not shown for clarity).

ingly it can predict $\alpha_p(\Delta p)$ and verify that the cake solids flux can be neglected.[20] For the model system used in these calculations, $\alpha_p(\Delta p)$ is shown in Figure 16. Note that it is a weak function of Δp.

The conventional theory of centrifugal filtration[28] yields

$$\frac{dv}{dt} = \frac{\frac{1}{2}\rho_l\omega^2(r_m^2 - r_f^2)}{\frac{\mu_f\phi_0\rho_s}{2\pi^2(r_m^2 - r_c^2)}\ln\left(\frac{r_m}{r_c}\right)\alpha_c v(t) + \frac{R_{mem}}{2\pi r_m}} \tag{71}$$

where μ_f is the fluid viscosity and the centrifugal cake resistance per unit mass of dry solids is denoted α_c.

Comparing with our compressional rheology result (Eq. 21) we see that, provided we can neglect the solids flux contribution (see below), the two expressions are equivalent if we make the identification:

$$\alpha_c = \frac{R^*}{\mu_f\rho_s\phi_0}\left\{\frac{Z_c(T)I_2[Z_c(T)]}{-\ln[1 - Z_c(T)]V(t)}\right\} \tag{72}$$

If the conventional model is valid, we should expect a close connection between α_c and $\alpha_p(\Delta p)$ but, unlike constant pressure filtration, the total pressure in centrifugal filtration varies across the cake and decreases monotonically in time. What, if any, connection does α_c have with $\alpha_p(\Delta p)$, and what Δp is relevant in centrifugal filtration? Our small time results (Eqs. 48 and 49) can be used to derive

$$\alpha_c(0) = \left(\frac{R^*}{\mu_f\rho_s\phi_0}\right)\frac{\lambda_g\phi_g\phi_0}{\phi_g - \phi_0}\left[1 + \frac{\frac{\Delta\rho}{\rho_l}\left(\frac{1}{\lambda_0 L}\right)}{1 + \frac{\Delta\rho}{\rho_l}\phi_0}\right] \tag{73}$$

The similarity solution for small time and zero membrane resistance gives

$$\alpha_c^{sim} = \frac{\gamma}{\beta}\int_0^1 d\eta\lambda[\Phi(\eta)]\Phi(\eta) \tag{74}$$

independent of T provided $Z_c \ll 1$.

The numerator of Eq. 71 in scaled terms is $P^*(L - V)$ and serves as an instantaneous driving pressure that we might wish to equate to $\Delta p/p_0$. Accordingly, in Figure 17, we plot $\alpha_c(t)$ calculated from Eq. 72 throughout a centrifugal filtration event from $t = 0$ to t_c. On the figure is also plotted $\alpha_p(P^*[L - V(t)])$ for $P^* = 100$. We note that $\alpha_c(t)$ is certainly not constant with time, first decreasing and then increasing to reach a roughly constant value for $t \approx t_l$. This plateau value may be compared to the similarity value for small membrane resistance values. We note that the similarity solution overpredicts the cake resistance.

The solids contribution to the total driving pressure is dominated by the sedimenting solids while they exist ($t < t_s$). In Figure 18 we plot the ratio of $I_3(Z_c)$ (the cake contribution) to the total solids contribution $(\Delta\rho/\rho_l)\phi_s(T)(Z_s - Z_c) + I_3(Z_c)$ as a function of $V(T)$ for various M and $P^* = 5$ to illustrate the relative contributions of sediment and cake.

While sedimenting solids exist the solids contribution to the driving pressure is about 15% of the fluid contribution, as can be seen in Figure 19, where we plot the ratio of solids contribution to fluid contribution as a function of expressed volume for various M and fixed $P^* = 5$. The ratio is insensitive to P*. As the sediment disappears this ratio becomes negligible and the fluid contribution (Z_f) becomes dominant.

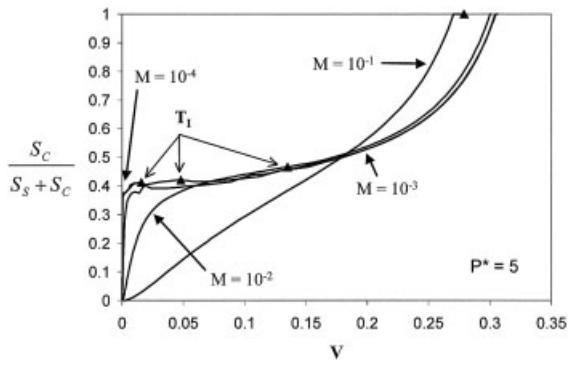

Figure 18. Ratio of the cake solids flux contribution to the total solids flux contribution for $0 < t \le t_s$ and $P^* = 5$.

The value at $V(T_l)$ is marked on each plot.

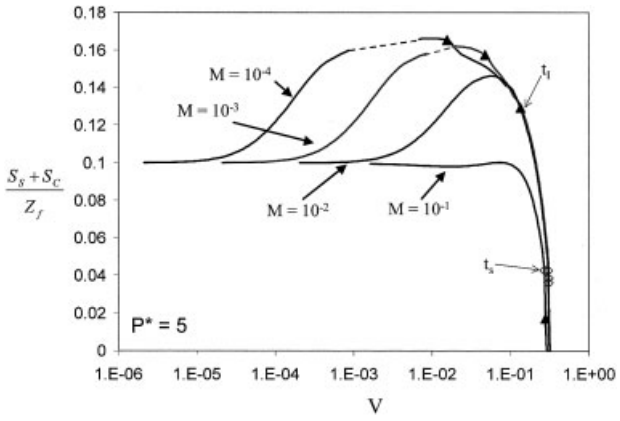

Figure 19. Solids flux contributions to $\dot{V}$ for P* = 5.

Conclusions

For the system conditions we have presented earlier, examining the time to the onset of immobilization (t_l) shows that the initial cake formation behavior is resolved in extremely short periods of time, fractions of a second for $\mathsf{M} < 10^{-2}$. It is therefore reasonable to assume that few, if any, experiments would be accurately described by the simple initial conditions we have used in these calculations. Drum spin-up and filter-loading rates are likely to have a significant effect on the initial cake formation behavior. So what utility do these calculations have? First, they show that the membrane resistance can control filtration rates for a significant portion of the total filtrate volume, if not filtration time. Figure 8 shows that for larger values of membrane resistance, more than a tenth of the total charged suspension can be expressed before cake immobilization sets in and the solids network controls the resistance to flow. Second, the membrane resistance affects the concentration profile. The concentration profile near the membrane is determined during the initial cake formation period and the resistance of the solids at the membrane will affect the rate of filtration and cake density as the filtration proceeds. Future models that take into account spin-up and loading rates will also have to take into account the membrane resistance–controlled portion of cake formation to accurately describe the solids network and thus the progress of filtration. We have also shown that the solids flux above a compressing cake should not be neglected when modeling batch centrifugal filtration.

In a companion article, we examine the cake compression and drainage stages for $T > T_c$ for our instantaneously loaded drum filter. The methods developed here should permit extension to the case where the loading is more gradual and also allow for drum spin-up.

Notation

$x^{(k)}$ = variable at time step k
D = diffusion coefficient
$I_1(Z)$ = integral of the solids volume over the range 0–Z
$I_2(Z)$ = integral of the resistance to flow resulting from solids over the range 0–Z
$I_3(Z)$ = integral of the contribution to the rate of expression arising from solids flux over the range 0–Z
L = scaled initial suspension volume (to be filtered) per unit length
M = membrane resistance divided by R_0
p_0 = prefactor for yield stress function
P^* = pressure scaling factor divided by p_0
p_l = liquid pressure
p_s = solids pressure
p_y = solids compressive yield stress
P_y = scaled solids compressive yield stress
q = scaled time derivative of solids concentration, $\Delta(\phi)(\partial\phi/\partial T)$
r = radial coordinate
r_m = radius of the filter drum
$R(\phi)$ = hydrodynamic resistance
R_0 = hydrodynamic resistance at infinite dilution
R^* = resistance scaling factor
R_{mem} = membrane resistance
$\boldsymbol{S}$ = suspension flux per unit area
S_c = scaled contribution of the flux of cake solids to the driving pressure
S_s = scaled sedimenting solids flux contribution to the driving pressure
t = time
t^* = timescaling
T = scaled time
t_l = time when the cake immobilizes at the membrane
t_s = time when the sedimenting solids have been collected into the cake
t_c = time when the liquid surface intersects the cake surface
$\boldsymbol{u}$ = solids velocity vector
v = volume expressed per unit length
V = scaled volume expressed per unit length
$\dot{V}$ = scaled rate of volume expression per unit length, dV/dT
$\ddot{V}$ = scaled rate of change of rate of volume expression per unit length, $\partial^2 V/\partial T^2$
$\boldsymbol{w}$ = liquid velocity vector
Z = scaled radial coordinate

Greek letters

α_p = cake resistance derived from pressure filtration modeling
α_c = cake resistance derived from centrifugal filtration modeling
β = V coefficient in similarity solution
γ = Z_c coefficient in similarity solution
η = similarity independent variable Z/Z_c
$\Delta(\phi)$ = scaled solids diffusion coefficient
ϕ = solids volume fraction
Φ = solids volume fraction in similarity solution
ϕ_I^0 = solids volume fraction at the membrane in the zero membrane resistance limit
ϕ_0 = solids volume fraction of the feed also initial solids concentration
ϕ_g = solids fraction at the gel-point
ϕ_{cap} = concentration where capillary stress equals the yield stress
ϕ^* = concentration at a comparison point
$\phi\boldsymbol{u}$ = solids flux
$\lambda(\phi)$ = scaled hydrodynamic resistance
μ = scaled membrane resistance
μ_f = suspension viscosity
ψ = scaled solids flux
ρ_l = liquid density
ρ_s = solids density
$\Delta\rho$ = solids density minus liquid density
ω = drum rotation rate (revolutions per second)

Literature Cited

1. Sambuichi M, Nakakura H, Osasa K, Tiller FM. Theory of batchwise centrifugal filtration. *AIChE J.* 1987;33:109-120.
2. Tiller FM, Hysung NB. Comparison of compacted cakes in sedimenting and filtering centrifuges. *Adv Filtr.* 1990;2:241-250.
3. Tiller F, Kirby MJM, Nguyen HL. Approximate theory for radial filtration/consolidation. *J Geotech Eng.* 1996;122:797-805.
4. Tiller FM, Kwon JH. Role of porosity in filtration: XIII. Behavior of highly compactible cakes. *AIChE J.* 1998;44:2159-2167.
5. Tiller FM, Li W. Comparing % cake solids in filtration, thickening, sedimenting centrifugation, and expression. *Fluid/Particle Sep J.* 1999;12:173-180.

6. Wakeman RJ. Modeling slurry dewatering and cake growth in filtering centrifuges. *Filtr Sep.* 1994;31:75-81.
7. Miller KT, Melant RM, Zukoski CF. Comparison of the compressive yield response of aggregated suspensions: Pressure filtration, centrifugation, and osmotic consolidation. *J Am Ceram Soc.* 1996;79:2545-2556.
8. Lee DJ, Ju SP, Kwon JH, Tiller FM. Filtration of highly compactible filter cake: Variable internal flow rate. *AIChE J.* 2000;46:110-118.
9. Zhao J, Wang C, Lee D, Tien C. Plastic deformation in cake consolidation. *J Colloid Interface Sci.* 2003;261:133-146.
10. Bürger R. Phenomenological foundation and mathematical theory of sedimentation–consolidation processes. *Chem Eng J.* 2000;80:177-188.
11. Bürger R, Concha F, Tiller FM. Applications of the phenomenological theory to several published experimental cases of sedimentation processes. *Chem Eng J.* 2000;80:105-117.
12. Bürger R, Evje S, Hvistendahl Karlsen K, Lie KA. Numerical methods for the simulation of the settling of flocculated suspensions. *Chem Eng J.* 2000;80:91-104.
13. Buscall R, White LR. The consolidation of concentrated suspensions. *J Chem Soc Faraday Trans 1.* 1987;83:873-891.
14. Buscall R, Goodwin JW, Ottewill RH, Tadros F. The settling of particles through Newtonian and non-Newtonian media. *J Colloid Interface Sci.* 1982;85:78-86.
15. Howells I, Landman KA, Panjkov A, Sirakoff C, White LR. Time-dependent batch settling of flocculated suspensions. *Appl Math Modell.* 1990;14:77-86.
16. Landman KA, White LR, Buscall R. The continuous-flow gravity thickener: Steady state behavior. *AIChE J.* 1988;34:239-252.
17. Landman KA, Russel WB. Filtration at large pressures for strongly flocculated suspensions. *Phys Fluids A.* 1993;5:550-560.
18. Landman KA, White LR. Determination of the hindered settling factor for flocculated suspensions. *AIChE J.* 1992;38:184-192.
19. Brown LA, Zukoski CF, White LR. Consolidation during drying of aggregated suspensions. *AIChE J.* 2002;48:492-502.
20. Landman KA, White LR, Eberl M. Pressure filtration of flocculated suspensions. *AIChE J.* 1995;41:1687-1700.
21. de Kretser RG, Usher SP, Scales PJ, Boger DV. Rapid filtration measurement of dewatering design and optimization parameters. *AIChE J.* 2001;47:1758-1769.
22. Landman KA, Sirakoff C, White LR. Dewatering of flocculated suspensions by pressure filtration. *Phys Fluids A.* 1991;3:1495-1509.
23. Williams WE. *Partial Differential Equations.* Oxford, UK: Clarendon Press; 1980.
24. Barr JD, White LR. Centrifugal drum filtration: II. A compression rheology model of cake draining. *AIChE J*. 2006;52:557–564.
25. Barr JD. *A Compression Rheology Model of Batch Centrifugal Filtration.* PhD Thesis. Pittsburgh, PA: Carnegie Mellon University; 2005.
26. Hairer E, Norsett SP, Wanner G. *Solving Ordinary Differential Equations 1. Nonstiff Problems*. 2nd Edition. Springer Series in Computational Mathematics. New York, NY: Springer-Verlag; 1993.
27. Shirato M, Sambuichi M, Kato H, Aragaki T. Internal flow mechanism in filter cakes. *AIChE J.* 1969;15:405-409.
28. McCabe WL, Smith JC, Harriott P. *Unit Operations of Chemical Engineering*. 5th Edition. New York, NY: McGraw-Hill; 1993.
29. Wakeman RJ, Tarleton ES. *Filtration: Equipment Selection, Modelling and Process Simulation.* London, UK: Elsevier Science; 1999.

Manuscript received Apr. 12, 2005, and revision received July 28, 2005.